Random anisotropy nematic model: Nematic–non-nematic mixture

V. Popa-Nita*
Faculty of Physics, University of Bucharest, P.O. Box MG-11, Bucharest 077125, Romania

Samo Kralj
Laboratory of Physics of Complex Systems, Faculty of Education, University of Maribor, Koroška 160, 2000 Maribor, Slovenia and Jožef Stefan Institute, Jamova 39, 1000 Ljubljana, Slovenia
(Received 7 December 2005; published 14 April 2006)

The influence of a random-anisotropy- (RA-) type disorder on the phase separation of the nematogen–non-nematogen mixture is studied. A combination of the phenomenological Landau–de Gennes and Flory-Huggins theories is used. We assume that the non-nematogen component (i.e., impurity) enforces the RA disorder to the enclosing thermotropic liquid-crystal (LC) phase. The Imry-Ma argument is used according to which the lower-temperature phase exhibits a domain-type pattern. The disorder strength is measured in terms of the dimensionless parameter Λ. We consider the case in which the LC molecules and impurities mix in the isotropic phase for $\Lambda=0$. The impurities enforce a finite degree of orientational ordering even in the high-temperature paranematic phase. In the low-temperature phase they give rise to a domain-type structure, resulting in the distorted nematic (speronematic) phase. We show that the onset of orientational ordering increases the phase separation tendency. The RA field, however, opposes this tendency. With increasing value of Λ the difference between the paranematic and speronematic ordering decreases. Consequently the structure of the phase-separated pattern can be much more complex in comparison to the $\Lambda=0$ case.

DOI: 10.1103/PhysRevE.73.041705 PACS number(s): 61.30.Dk, 61.30.Hn, 64.75.+g

I. INTRODUCTION

For years there has been an intense interest in behavior of disordered liquid-crystal (LC) phases [1,2]. These systems play an important role in various electro-optic applications and are also of interest for basic science. Namely, they exhibit many universalities [3] that link them mathematically with other (often completely different) physical systems. These universalities can be experimentally relatively easily studied [4] in LC's mainly due to their fluidity, softness, and optic transparency and anisotropy.

In perturbed LC's, disorder is mostly introduced geometrically via a spatially randomly varying liquid-crystal–perturber interface [1]. For perturbers one commonly chooses inert porous matrices hosting LC phases or networks formed by aerosil particles in aerosil–liquid-crystal mixtures. As matrices, aerogels [5,6], Russian glasses [7], Vycor glasses [8], and controlled-pore glasses [9,10] are conventionally used. Aerosil mixtures [11,12] are particularly adequate because one can obtain qualitatively different random-field-type regimes by changing the concentration of aerosil particles.

In these systems the combined action of finite-size effects, surface interactions, and randomness has to be taken into account. The finite-size effects are strongly apparent in the specific-heat scaling behavior at the second order N-SmA phase transition [10,11]. The LC-perturber interfaces by themselves (i.e., for small enough interface curvature with respect to the relevant LC order-parameter correlation length) commonly tend to increase the local degree of LC ordering. Consequently in such samples at interfaces the degree of ordering could be increased [9,10] or even apparent prewetting phenomena [10,13,14] can take place. On the other hand, the randomness works against the interface ordering tendency. It also globally enforces the isotropic distribution of the relevant LC (quasi-)long-range-ordering field. In the case of nematic and smectic phases these (also called hydrodynamic) fields correspond to the nematic director and smectic layer phase fields, respectively. Several studies suggest that the randomness gives rise to a domain-type ordering [5,15–18], which is for a weak enough disorder characterized by a single representative domain length ξ_d. Such domain patterns were first predicted by Imry and Ma [19] in magnetic systems. The so-called Imry-Ma argument [19] claims that an arbitrary weak disorder breaks the system into a domainlike pattern. The necessary conditions are that (i) the system possess a Goldstone mode (i.e., the phase is reached via a continuous symmetry breaking phase transition) and (ii) the spatial dimension d be equal or less than 4. Consequently the (quasi-)long-range ordering of the pure system is replaced by a short-range ordering. The characteristic domain size ξ_d is expected to scale as $\xi_d \propto w^{-2/(4-d)}$, where w measures the disordering strength. Some authors predict instead the onset of quasi-long-range order [20,21], characterized by algebraically decaying correlations. Note that also in this case ξ_d plays a significant role measuring the distance above which the correlations decay rather weakly [22].

In some cases the perturbers are mobile and the phase separation can take place. This phenomenon in combination with randomness has not yet been studied systematically. Note that high-precision calorimetric studies [11,23] of LC-aerosil mixtures at the isotropic-nematic phase transition report a bimodal behavior. A possible explanation of this ob-

*Author for correspondence. Electronic address: v.popanita@gmail.com

 ©2006 The American Physical Society

servation is the phase separation. In this respect we refer to recent studies [24,25] in which nematogen–non-nematogen mixtures were studied. For the isotropic interaction between unlike molecular species either the Carnaham-Starling [26] approach of a hard-sphere suspension [24] or the Flory-Huggins approach [27] was used [25]. For both approaches it has been shown that a biphasic region between the isotropic and nematic phases appears below the nematic-isotropic transition temperature of the pure thermotropic nematogen.

In this paper we extend our previous studies [15–18,25,28] on randomly perturbed nematic phases, emphasizing the influence of disorder on phase separation of a binary nematic–non-nematic mixture. We assume that the impurities (i.e., the non-nematic component) via the impurity-LC interface orientational anchoring interaction impart to the LC phase a kind of random anisotropy field [15,29]. We use a combination of the random anisotropy nematic (RAN) [15] and Flory-Huggins [27] models. We study the phase stability of the mixture as a function of the absolute temperature T, impurity concentration c, and random anisotropy field strength Λ. We show that the random anisotropy field even qualitatively changes the topology of the (c,T) phase diagram. We emphasize the following main differences with respect to the $\Lambda=0$ case: (i) the phase separation in the suppressed, and (ii) the structure of bistable region becomes more complex.

The paper is organized as follows. In the next section we introduce the model we use. The results concerning the influence of disorder are presented in Sec. III. In the last section we summarize and discuss our results.

II. MODEL

In our calculations we use the phenomenological random anisotropy nematic model [15]. The introduction of this model was inspired by the semimicroscopic random anisotropy magnetic (RAM) [29] lattice model, used to study a class of randomly perturbed magnetic systems. In the following we first introduce the lattice RAM and RAN models. Then we express the free energy of the binary nematic–non-nematic mixture using the Landau–de Gennes [30] and Flory-Huggins [27] approaches. We consider the uniaxial nematic ordering and introduce the effective description of the system. We assume that the impurities affect the orientational LC ordering via a random-anisotropy-type field, whose strength is measured with the dimensionless constant Λ.

A. Random anisotropy nematic lattice model

The RAM lattice Hamiltonian [29] is expressed as

$$H = -\frac{1}{2}\sum_i \sum_j J_{ij}\mathbf{s}_i \cdot \mathbf{s}_j - \sum_i w_i(\mathbf{s}_i \cdot \mathbf{e}_i)^2. \tag{1}$$

Here $\mathbf{s}_i$ stands for an n-component spin at the ith site in a d-dimensional lattice. The sums in Eq. (1) run over all lattice sites. The quantity J_{ij} describes the magnetic interaction between the ith and jth spin. For the ferromagnetic short-range interaction one sets $J_{ij}=J>0$ for the first neighbors and $J_{ij}=0$ elsewhere. A positive constant w_i stands for the local field strength at the ith site. It forces $\mathbf{s}_i$ locally along $\pm\mathbf{e}_i$, the orientation of which varies randomly from site to site.

The analogous RAN lattice free energy can be expressed as

$$F = -\frac{1}{2}\sum_i \sum_j J_{ij}(\mathbf{n}_i \cdot \mathbf{n}_j)^2 - \sum_i w_i(\mathbf{n}_i \cdot \mathbf{e}_i)^2. \tag{2}$$

Here $\mathbf{n}_i$ is the unit vector pointing along the average orientation of a rodlike LC molecule at the ith site of a lattice. The average orientation of $\mathbf{n}_i$ over a few simulation cycles roughly corresponds to the nematic director field $\mathbf{n}$ in the continuum picture. Linear terms in the unit vector field $\mathbf{n}_i$ in Eq. (2) are not allowed because of the head-to-tail (i.e., $\mathbf{n}_i \rightarrow -\mathbf{n}_i$) invariance of LC molecules. The interaction J_{ij} is commonly taken to be short ranged. Therefore $J_{ij}=J>0$ is different from zero only between the first neighbors. In the second term in Eq. (2) the unit vector field $\mathbf{e}_i$ randomly orientationally varies from site to site. This orientation is locally enforced to a LC molecule if $w_i>0$. In typical simulations [20,31] the random anisotropy field strength is set to a constant positive value $w_i=w$ at a fraction p of all sites and $w_i=0$ elsewhere, as in the RAM analog.

The limit $w=0$ of the RAN model is referred to as the Lebwohl-Lasher [32] model. It reasonably describes the temperature-driven isotropic-nematic phase transition. In the continuum limit it maps to the so-called Frank free-energy expression in the approximation of equal Frank nematic elastic constants [30,33]. Note that the case for a finite value of w was treated by several authors, but different conclusions were reached about the character of the resulting nematic ordering [20,21,31].

B. Free energy

We analyze the influence of disorder on phase diagram of the thermotropic nematic–non-nematic binary mixture at an intermediate scale (mesoscopic scale). The mixture is characterized by a conserved parameter and a nonconserved parameter. The conserved parameter is the concentration $c=N_1/N$ of the impurities (the non-nematic component), where N_1 is the number of impurity molecules and N stands for the total number of molecules. The nonconserved parameter is the orientational nematic order parameter $Q_{\alpha\beta}$, which is a traceless symmetric second-rank tensor. In case of uniaxial nematic states, the local orientational ordering can be expressed as [30,33]

$$Q_{\alpha\beta} = S(3n_\alpha n_\beta - \delta_{\alpha\beta})/2. \tag{3}$$

The unit vector $\mathbf{n}$, referred to as the nematic director field, points along the average local uniaxial orientation of LC molecules. Due to the head-to-tail invariance of LC molecules, the cases $\pm\mathbf{n}$ refer to the same state. The scalar S is the orientational order parameter. The isotropic liquid is characterized by $S=0$, and a rigidly oriented nematic phase (i.e., no fluctuations about $\mathbf{n}$) would be characterized by $S=1$.

We express the free energy F of the mixture as the sum of volume f_V and interface f_i contributions:

$$F = \int\int\int f_V dV + \int\int f_i dA, \tag{4}$$

where V is the volume of the system and A stands for the surface area of the LC-impurity interface.

We express the volume term as

$$f_V = f_m(c) + (1-c)[f_c(c,Q_{\alpha\beta}) + f_e(Q_{\alpha\beta,\gamma})]. \tag{5}$$

The first term is the free-energy density of the isotropic mixing for the two components [27]

$$f_m(c) = \frac{Nk_BT}{V}[(1-c)\ln(1-c) + c\ln c + \chi c(1-c)]. \tag{6}$$

Here k_B is the Boltzmann constant and $\chi=(U_0/k_bT)$ is the Flory-Huggins interaction parameter related to isotropic interaction between unlike molecular species [27].

The second term in Eq. (5) is the Landau–de Gennes free-energy density condensation [30,33]

$$f_c(c,Q_{\alpha\beta}) = (1-c)\{a[T-(1-\lambda c)T^*]Q_{\alpha\beta}Q_{\beta\alpha} - BQ_{\alpha\beta}Q_{\beta\gamma}Q_{\gamma\alpha} + C(Q_{\alpha\beta}Q_{\beta\alpha})^2\}. \tag{7}$$

The coupling between c and $Q_{\alpha\beta}$ in Eq. (7) results from microscopic considerations. According to Humphries-James-Luckhurst theory on a binary mixture [34], the orientational free energy per molecule in a mean-field approximation is given by

$$f/Nk_BT = -\frac{(1-c)^2uS^2}{2} + (1-c)\int f(\beta)\ln f(\beta)\sin\beta d\beta, \tag{8}$$

where the strength of the molecular field is determined by the molecular anisotropy u, β is the angle between the symmetry axis of the (cylindrically symmetric) molecule and the director, and $f(\beta)$ is the singlet orientational distribution function. The first term is the internal energy per molecule, while the second one represents the decrease of entropy due to the nematic ordering. The free energy given in Eq. (8) can be compared with the Landau–de Gennes expansion [35]. The consequence is that only the T^* term in the Landau–de Gennes free energy comes from the internal energy, while the other terms result from the entropy expansion.

The elastic part $f_e(Q_{\alpha\beta,\gamma})$ of the free-energy density opposes spatial variations in $\mathbf{Q}$ and can be expressed in the simplest form as [30,33]

$$f_e(Q_{\alpha\beta,\gamma}) = LQ_{\alpha\beta,\gamma}Q_{\alpha\beta,\gamma}, \tag{9}$$

where L is a representative bare nematic elastic constant. In the Frank description of the nematic ordering only in terms of $\mathbf{n}$ does this form of f_e correspond to the approximation of equal Frank elastic constants.

The most essential orientational anchoring ordering term in the interface free-energy density in Eq. (4) can be expressed as [36]

$$f_i(Q_{\alpha\beta}) = -\frac{W}{3}e_\alpha Q_{\alpha\beta}e_\beta, \tag{10}$$

where W is the positive anchoring strength constant tending to align the LC molecules along the unit vector $\mathbf{e}$, referred to as the easy axis of the LC-impurity interface.

For a pure uniaxial nematogen the condensation free-energy density has the form

$$f_c(S) = \frac{3}{2}a(T-T^*)S^2 - \frac{3}{4}BS^3 + \frac{9}{4}CS^4. \tag{11}$$

This term drives the first-order nematic-isotropic phase transition. In the case of spatially homogeneous LC ordering the nematic $[S_n \equiv S(T_{IN}) = B/6C]$ and isotropic $(S=0)$ phases coexist in equilibrium at the phase transition temperature $T=T_{IN}=T^*+B^2/24aC$. The undercooling limit temperature of the isotropic phase is labeled with T^*.

The most essential elastic and interface free-energy density terms in the uniaxial description of a pure nematogen are expressed as

$$f_e = \frac{3L}{2}|\nabla S|^2 + \frac{9L}{2}S^2|\nabla \mathbf{n}|^2, \tag{12}$$

$$f_i = -\frac{W}{2}S\left((\mathbf{n}\cdot\mathbf{e})^2 - \frac{1}{3}\right). \tag{13}$$

C. Mesoscopic random anisotropy nematic approach

If a relatively weak disorder is enforced on a liquid-crystal phase, according to the Imry-Ma theorem [19], the competition between the elastic ordering and random field disordering tendencies results in a domainlike pattern. This pattern is characterized by a single length scale ξ_d. We accept this prediction and treat ξ_d as the variational parameter. The remaining two variational parameters in our approach are the average nematic order parameter $\langle S\rangle$ and the average impurity concentration $\tilde{c}=\langle c\rangle$. Here $\langle\cdots\rangle$ denotes the averaging within the domain volume $V_d \sim \xi_d^3$.

In the following we explain how ξ_d enters into the effective form of the free-energy density $\langle f\rangle = \langle F_d\rangle / V_d$ [15,18], where $\langle F_d\rangle$ stands for the average free-energy density within the average domain. The RAN-type disordering field enters in F via the interface contribution given by Eq. (13). We consider cases where $\mathbf{e}$ exhibits random variations. In real samples this can be caused by a predominantly randomly spatially varying LC-impurity interface orientation. The reason behind this might also be randomly placed impurities, which will be discussed in more details in the Conclusions. We also assume that the surface-to-volume ratio of the liquid-crystal phase is relatively high and nearly homogeneously distributed over the system volume.

In the spirit of the RAN approach we set that the easy axis $\mathbf{e}$ randomly spatially varies within a typical domain. To estimate the averaging rate within it we introduce the distance ξ_r on which $\mathbf{e}$ significantly changes. Thus, on traversing the domain volume, the liquid-crystal molecules experience $N_d \sim (\xi_d/\xi_r)^3$ random changes. For an infinitely large cluster

(i.e., $N_d \to \infty$) and for essentially homogeneously oriented $\mathbf{n}$ along a symmetry breaking direction within the domain, the term $[(\mathbf{n}\cdot\mathbf{e})^2 - 1/3]$ averages to zero. For a finite value of N_d, according to the central limit theorem, the averaging effectiveness is proportional to $1/\sqrt{N_d}$. It follows that

$$\left\langle (\mathbf{n}\cdot\mathbf{e})^2 - \frac{1}{3} \right\rangle \sim \frac{1}{\sqrt{N_d}} \sim \left(\frac{\xi_r}{\xi_d}\right)^{3/2}. \tag{14}$$

Using this approximation we express the average interface free-energy density $\langle f_i \rangle$ as

$$\langle f_i \rangle \sim -\frac{W\langle S\rangle}{2}\left(\frac{\xi_r}{\xi_d}\right)^{3/2}, \tag{15}$$

where $\langle S \rangle$ stands for the average value of S within the domain. We also assume that the relative importance of the interface free-energy density term in $\langle f \rangle$ is proportional to $c(1-c)$. The linear dependence on c is due to the fact that the impurities are the origin of the random-field-type distortions. The $(1-c)$ contribution arises because all the relative importance of the LC component in the system is proportional to $(1-c)$.

In general the scale ξ_r on which the local anisotropy axis changes depends on the impurity concentration. Due to simplicity, we do not take this into account. This is justified for cases where $\xi_r \ll \xi_d$. This is also the limit in which the central limit approximation is sensible.

The interface term enforces $\xi_d \to 0$. The elastic term, which roughly scales with ξ_d as [15]

$$\langle f_e \rangle \sim \frac{9}{2} L \langle S \rangle^2 \frac{1}{\xi_d^2}, \tag{16}$$

opposes this tendency, favoring $\xi_d \to \infty$.

D. Dimensionless free-energy density

For convenience we introduce the following ratios and nondimensional quantities. The orientational order parameter is normalized with respect to its value at the pure bulk phase transition—i.e., $\tilde{S} = S/S_n$—$\tau = (T - T^*)/(T_{IN} - T^*)$ is the reduced temperature, κ and Λ are the dimensionless elastic constant and dimensionless anchoring strength, and $\tilde{f} = \langle f \rangle / f_0$ is the dimensionless free-energy density, where $f_0 = B^4/24^2C^3$. For numerical purposes we introduce instead of ξ_d the dimensionless length $\xi = \sqrt{\xi_d^2/\xi_r^2 - 1}$. Therefore the case $\xi = 0$ corresponds to $\xi_d = \xi_r$.

Omitting the tildes, the nondimensional free-energy density f becomes

$$f = f_h + (1-c)(f_e + f_i). \tag{17}$$

The dimensionless homogeneous (f_h), elastic (f_e), and interface (f_i) terms are expressed as

$$f_h = \Gamma[(1-c)\ln(1-c) + c\ln c + \chi c(1-c)] + (1-c)[(\tau + \lambda c)S^2 - 2S^3 + S^4], \tag{18}$$

$$f_e = \frac{\kappa S^2}{1+\xi^2}, \tag{19}$$

$$f_i = -\frac{c\Lambda S}{(1+\xi^2)^{3/4}}, \tag{20}$$

where $\Gamma = Nk_BT/Vf_0$ and $\lambda = 24aCT^*/B^2$. Now, for a pure bulk nematogen the phase transition temperature is $\tau_{IN} = 1$, $S(\tau_{IN}) = 1$, and $\tau = 0$ corresponds to the undercooling limit temperature of the isotropic phase.

Note that the local ordering tendency of impurities for $\Lambda > 0$ induces a finite value of S even at relatively high temperatures (i.e., at $\tau > 1$). One commonly refers to such a case as *paranematic* ordering. The equilibrium condition at the nematic-paranematic phase transition is given by the following set of equations [37]:

$$\Delta g(c,S) = 0, \quad \frac{\partial \Delta g}{\partial c}(c,S) = 0, \quad \frac{\partial \Delta g}{\partial S}(c,S) = 0, \tag{21}$$

where

$$\Delta g(c,S) = f(c,S) - f(c_p,S_p) - \mu(c - c_p) \tag{22}$$

is the difference in grand potential density between the two phases and

$$\mu = \frac{\partial f}{\partial c}(c_p,S_p) \tag{23}$$

is the chemical potential. The ordering in the nematic and paranematic phases is determined by the pairs (c,S) and (c_p,S_p), respectively.

Our purpose is to calculate the stability phase diagram in the (c,T) plane as a function of Λ. We calculate the paranematic-nematic coexistence curve (binodal) numerically by finding pairs of states with equal chemical potentials and pressures. This is equivalent to the minimization of Δg with respect to the nonconserved order parameter S, followed by a common tangent to a pair of points on the curve $f(c)$ [37].

III. PHASE BEHAVIOR

Using the described model we calculate numerically the phase behavior of the system as a function of the dimensionless temperature τ, impurity concentration c, and random field strength Λ.

A. Undistorted bulk sample

We first consider a bulk sample where the elastic and interface terms are absent (i.e., $f_i = f_e = 0$, which is equivalent to setting $f = f_h$). In this case the paranematic phase is replaced by the isotropic one and $S_p = S_i \equiv 0$, where S_i stands for the degree of ordering in the isotropic phase. Taking into account Eqs. (21) we calculate a representative phase diagram of the nematic-impurity (i.e., nematic–non-nematic) mixture, which is plotted in Fig. 1. The solid curve refers to the binodal (which constitutes the actual phase boundary), and the dotted lines show the hidden first-order nematic-isotropic transition, where the isotropic and nematic branches of the grand potential are equal. The dash-dotted lines are the spinodals. For temperatures below T_{NI} $(\tau_{NI} = 1)$,

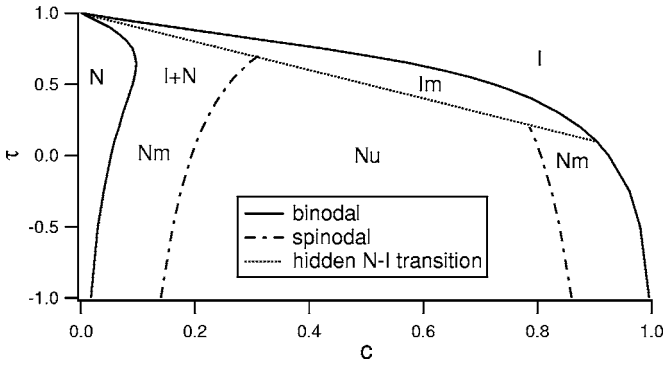

FIG. 1. Phase diagram for the nematic–non-nematic binary mixture in the absence of disorder. The solid curve refers to the binodal, the dotted line shows the hidden nematic-isotropic phase transition, and the dashed-dotted line is the spinodal. $\Gamma=\lambda=\chi=1$. Below $\tau=\tau_{NI}=1$, a region of two-phase (I+N) coexistence exists between isotropic (I) and nematic (N) phases. The undercooling limit temperature for the isotropic phase T^* in the pure nematogen corresponds to $\tau^*=0$.

there exists a two-phase coexistence region (I+N) between the isotropic (I) and nematic (N) phases. On decreasing the temperature the biphasic region broadens. Within the biphasic region there are two different metastable regions: an isotropic metastable (Im) and a nematic metastable (Nm) region, as well as an unstable region of the nematic (Nu).

We further emphasize that the phase diagram in Fig. 1 is plotted for the following values of the important parameters: $\chi=\Gamma=1$. For this choice the value of χ is below the critical value $\chi_c=2$ [38]. For $\chi>\chi_c$ the phase separation takes place even in the isotropic phase.

To show how the onset of nematic ordering triggers phase separation in conventional LC's, we rewrite f [see Eq. (18)] in the following form:

$$f=\Gamma[(1-c)\ln(1-c)+c\ln c+\chi_{eff}c(1-c)] + (1-c)(\tau_{eff}S^2-2S^3+S^4), \tag{24}$$

where $\tau_{eff}=\tau$ and χ_{eff} stands for the effective Flory-Huggins interaction parameter:

$$\chi_{eff}=\chi+\frac{\lambda S^2}{\Gamma}. \tag{25}$$

We see that the nematic ordering effectively increases the Flory-Huggins interaction parameter, which can potentially lead to order-induced phase separation.

B. RAN phase behavior

To see the impact of RAN ($\Lambda>0$), we rewrite f in the form given by Eq. (24). It follows that

$$\chi_{eff}=\chi+\frac{1}{\Gamma}\left(\lambda S^2-\frac{\Lambda S}{(1+\xi^2)^{3/4}}\right), \tag{26}$$

$$\tau_{eff}=\tau+\frac{\kappa}{1+\xi^2}. \tag{27}$$

Therefore, the random field tends to suppress the phase separation for a finite value of ξ. In the $\Lambda=0$ case in the nematic phase the onset of orientational ordering increases the difference between the nematic and non-nematic molecules. Consequently the phase separation tendency is increased. The presence of the RAN field via its averaging influence decreases this difference, reducing the phase separation tendency. On the contrary the local ordering tendency of the RAN field could also trigger phase separation in the paranematic phase (where $S=S_p>0$) if $\chi_{eff}>2$. We mention that the phase separation in the presence of a random field takes place between the paranematic and speronematic phases. The paranematic phase closely resembles the isotropic phase but exhibits a finite degree of nematic ordering and $\xi=0$. The speronematic phase represents a distorted nematic phase that is characterized by a finite value of ξ (for an ordinary nematic phase $\xi\to\infty$).

To show further qualitative influences of Λ we study its influence on phase behavior numerically. In order to simplify the numerical procedure we discard the linear $f_i\propto c$ dependence in Eq. (20). We set instead $f_i=-\Lambda S/(1+\xi^2)^{-3/4}$. Therefore we assume that the strength of the RAN field is independent of c. Our tests show that in the region of interest this change does not induce qualitative changes in the studied phase behavior.

Minimizing Eq. (17) with respect to ξ leads to

$$\xi=\begin{cases}0 & \text{when } S<S_c,\\ \left[\left(\dfrac{S}{S_c}\right)^4-1\right]^{1/2} & \text{when } S>S_c,\end{cases} \tag{28}$$

where $S_c=3\Lambda/4\kappa$. The corresponding free-energy density is given by

$$f(c,S)=\begin{cases}f_p(c,S)=f_h(c,S)-\Lambda S+\kappa S^2 & \text{when } S<S_c,\\ f_s(c,S)=f_h(c,S)-\dfrac{27}{256}\left(\dfrac{\Lambda}{\kappa}\right)^4S^{-2} & \text{when } S>S_c.\end{cases} \tag{29}$$

The subscripts p and s stand for *paranematic* and *speronematic* ordering, respectively.

To calculate the phase diagram we use the equilibrium conditions given by Eqs. (21). The solution of these equilibrium conditions is determined by four quantities: (i) the paranematic phase is determined by c_p and S_p and (ii) the speronematic phase by c_s and S_s.

The phase (τ,Λ) phase diagram for $\kappa=1$ is presented in Fig. 2. There are two different solutions of equilibrium conditions (21). For $0<\Lambda<\Lambda_*$, the stable solution (which we have labeled *solution I*) develops from the bulk solution (in the absence of disorder). It predicts phase separation with different values of concentrations and orientational order parameters in the paranematic and speronematic phases. It is characterized by a relatively large difference in concentrations between the two phases (close to the difference in concentrations predicted by the bulk solution). At $\Lambda=\Lambda_*$ this

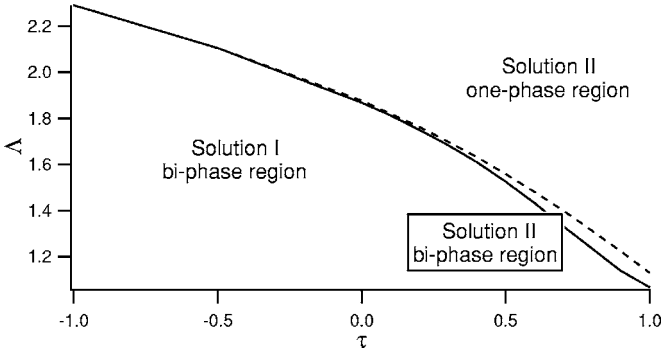

FIG. 2. The influence of disorder on the phase separation for the nematogen–non-nematogen binary mixture. The phase diagram (τ,Λ) contains three distinct regions. Region I: *solution I* which predicts the phase separation is stable. Region II: *solution II* which predicts a different phase separation becomes stable. Region III: *solution II* is stable in which the speronematic and paranematic orderings (i.e., $S_s=S_p$, $c_s=c_p$) are equal. Therefore in this region a homogeneous mixture exists. Solid line: $\Lambda_*(\tau)$. Dashed line: $\Lambda_c(\tau)$.

solution becomes metastable and the other solution of equilibrium conditions (21) becomes stable (which we have labeled *solution II*). This second solution, which predicts the cancellation of phase separation, is characterized by two different behaviors: (i) for $\Lambda_*<\Lambda<\Lambda_c$, it predicts a phase separation but with a smaller difference in concentrations between the two phases, comparatively with *solution I*, and (ii) at even larger degree of disorder $(\Lambda>\Lambda_c)$, this second solution is still stable but it does not predict anymore a phase separation. To sum up, the two characteristic values of the disorder, $\Lambda_*(\tau)$ and $\Lambda_c(\tau)$, define two curves in (τ,Λ) space. At low values of disorder, a solution develops from the bulk solution, which predicts a phase separation. At intermediate values of disorder, the first solution becomes metastable and another solution becomes stable, which predicts a phase separation with a smaller difference in concentration. At large degree of disorder, this second solution remains stable

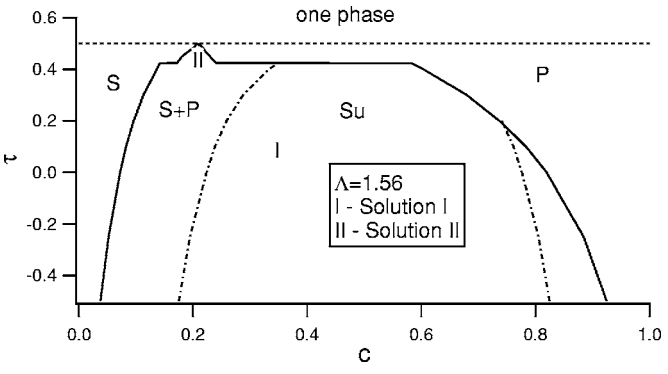

FIG. 3. The phase diagram of the nematogen–non-nematogen binary mixture for $\Lambda=1.56$. The paranematic and speronematic phases are labeled with *P* and *S*, respectively. The solid curve refers to the binodal, and the dashed-dotted line is the spinodal. Region I: *solution I* is stable. Region II: *solution II* (with a smaller concentration difference $\Delta c=c_p-c_s$) is stable. For $\tau>0.5$ the two phases have the same concentrations and order parameters. $\Gamma=\lambda=\chi=\kappa=1$.

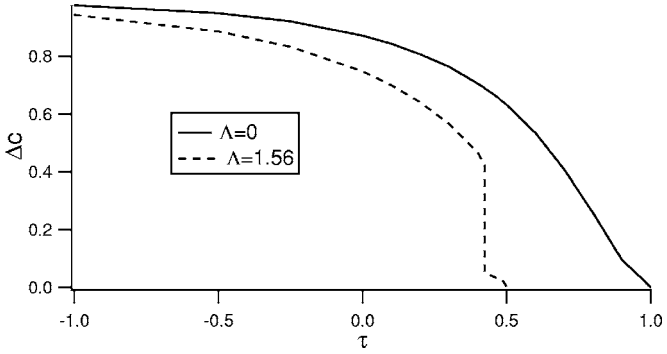

FIG. 4. The difference of concentrations, $\Delta c=c_p-c_s$, between the two phases as a function of temperature. Solid line: $\Lambda=0$. Dashed line $\Lambda=1.56$. $\Gamma=\lambda=\chi=\kappa=1$.

but now it does not predict a phase separation. The critical value of disorder Λ_c, at which the phase separation is canceled, increases with decreasing temperature. This can be explained by the fact that with decreasing temperature, the difference in concentrations between the two phases increases. Thus a larger degree of disorder is needed to cancel it.

A demonstrative phase diagram of the system for a fixed degree of disorder $(\Lambda=1.56)$ is shown in Fig. 3. In *region I*, at low temperatures $(\tau<0.4)$, *solution I* is stable. At $\tau=0.4$ the transition into *region II* takes place. Finally, for $\tau>0.5$ *region III* is entered. In it *solution II* consists of only one phase (i.e., the paranematic and speronematic phases are identical).

The difference of concentration between the speronematic and paranematic phases for two different values of Λ is plotted as a function of temperature in Fig. 4. The disorder has two main effects. (i) It induces smaller concentration differences between the paranematic and speronematic phases. (ii) It gives rise to an additional solution. This is manifested by the jump of $\Delta c=c_p-c_s$ at $\tau=0.4$, corresponding to the transition between solutions I and II.

The corresponding difference $\Delta S=S_s-S_p$ of the order parameters between the speronematic and paranematic phases is plotted in Fig. 5. The disorder (dashed line) induces a smaller jump of the order parameter at the transition. This jump is nearly constant with reducing temperature in solution II.

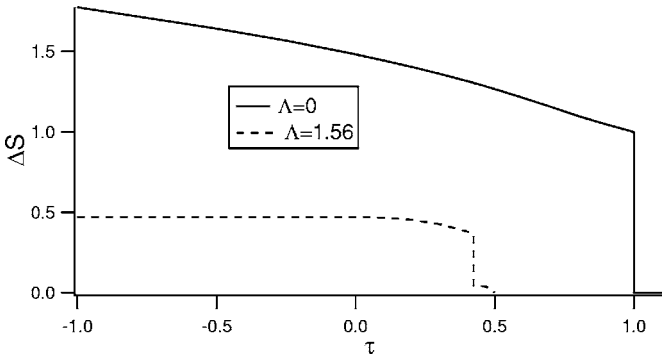

FIG. 5. The difference of order parameters, $\Delta S=S_s-S_p$, between the two phases as a function of temperature. Solid line: $\Lambda=0$. Dashed line $\Lambda=1.56$. $\Gamma=\lambda=\chi=\kappa=1$.

IV. CONCLUSIONS

We study the influence of the RAN-field-type disorder on the phase separation of the nematogen–non-nematogen mixture. We focus on the paranematic-speronematic coexistence. The speronematic ordering refers to the distorted nematic phase, characterized by a finite value of ξ. The non-nematogen component is treated as an impurity that enforces the RAN field to the enclosing LC molecules. In calculations we use a combination of the Landau–de Gennes approach [30,33] in terms of the uniaxial tensor order parameter and the Flory-Huggins approach [25,27]. The latter is used to study the phase separation of a mixture of unlike molecules that interact via an isotropic interaction. The form of the coupling between the nematic order parameter S and the concentration c of impurities is suggested by microscopic considerations [25,34].

Following the Imry-Ma prediction [19,15] we assume that the system breaks into a domain-type pattern, which is characterized by the average domain size length ξ. A finite value of ξ results from the interplay between the (i) elastic interactions and (ii) RAN field, favoring (i) $\xi \to \infty$ and (ii) $\xi \to 0$, respectively. We measure the relative strength of the RAN field in terms of the dimensionless constant Λ. We construct the effective free energy of the system, which depends on the following set of variational fields: S, c, and ξ.

We first consider the case without the RAN field (i.e., $\Lambda=0$). We show that the onset of nematic ordering for conventional LC material parameters strongly increases the effective Flory-Huggins parameter χ_{eff}. Therefore in the nematic phase the phase separation is expected even if in the isotropic phase the value of χ_{eff} is below the critical value χ_c.

We further show that the RAN field suppresses the phase separation tendency. We demonstrate that the RAN field increases the complexity of the LC-impurity configuration if the phase separation nevertheless takes place. This is mainly due to the decreased difference between the paranematic and speronematic phases for $\Lambda>0$ in comparison to the difference between the nematic and isotropic phases for $\Lambda=0$. To illustrate that we considered the case with $\chi=1<\chi_c$ for $\Lambda=0$ and $\Lambda>0$. For $\Lambda=0$ the phase separation solution (to which we refer as solution I) is determined by the coexistence of the isotropic and nematic components, characterized by the following sets of parameters: $(S=S_i\equiv 0, c=c_i)$ and $(S=S_n, c=c_n)$ where $c_n<c_i$ and $\chi_{eff}(S=S_n)>\chi_c$. For $\Lambda>0$ the value of χ_{eff} is affected by LC ordering also in the paranematic phase. Therefore, phase separation could be triggered in both speronematic and paranematic phases. Consequently we obtain for the chosen set of parameters at the speronematic and paranematic coexistence two different solutions (solutions I and II). The relative stability of these solutions for a given value of Λ depends on the temperature.

We emphasize that our approach is approximative, yielding qualitative predictions on the influence of disorder on phase separation. In the following we discuss some of the limitations of our model, analogies, and the relation with experimental systems.

Our approach assumes a domain-type orientational structure that is well characterized by a single characteristic length scale. Note that a single-length-scale domain pattern temporally arises also in a fast enough isotropic quench [39]. In the scaling regime the characteristic domain size of the resulting pattern grows exponentially with time. In an impure sample this pattern could be pinned and stabilized by impurities. If the disorder strength is not strong enough, the distribution of ξ_d values is not substantially broadened. This domain pattern resembles the one that we consider in our model. Such a pattern does not exhibit relatively thin walls as encountered in a typical ferromagnetic domain structure. With respect to magnetic analogs it is closer to the correlated spin-glass structure [40] in which the magnetization varies more or less smoothly over the sample.

In our approach the impurities (the non-nematogen component) enforce a static random-anisotropy-type disorder to surrounding LC molecules. We assume that the system is close to thermal equilibrium (i.e., locked in a relatively deep metastable glassy state). In a real sample these impurities could move, making a time-dependent disorder field, which is not taken into account in our model. However, we believe that the mobility of impurities does not cause apparent changes on the macroscopic scale if the system is close to equilibrium. The impurities in our model affect the LC orientational ordering. The mediating nematic director field gives rise to relatively long-range interactions among impurities. Consequently a move of an impurity is in general not a local event like in a conventional liquid. It is very unlikely that the movement of an impurity would trigger a relatively large rearrangement of the system from the orientational point of view because this requires energy.

From the experimental point of view the system we study well mimics the LC-aerosil mixtures [11]. The hydrophilic spherular aerosil particles of diameter 7 nm enforce a homeotropic (i.e., orientation along the particle surface normal) anchoring to surrounding liquid-crystal molecules. These mixtures are believed to be adequate model systems for random-field-type disorder [2,11,12,41,42]. By varying the concentration ρ_s of aerosil particles different types of disorder regimes are realized. Particularly interesting is the so-called soft regime [11] that roughly extends in the interval $0.01\ \mathrm{g/cm^3}<\rho_s<0.1\ \mathrm{g/cm^3}$. In this regime the aerosils form a weakly connected network gel of thixotropic character [11]. This adaptive network, which is well characterized by a single length scale $l_0 \propto 1/\rho_s$, enforces on LC molecules a kind of random field. Further the network can reshape in order to relieve the large enough elastic strain imposed by a surrounding LC phase. We emphasize that in aerosil-LC mixtures the random spatial variation of the random field orientation arises due to the essentially random structure (i.e., the positions of spherular aerosil particles) of the aerosil network. Note that several observations [11,41,42] report a double-peak specific-heat appearance at the isotropic– (i.e., paranematic-) nematic (i.e., speronematic) phase transition. Mercuri *et al.* [41] explain it by claiming that this reflects the transition between so-called random dilution to the quenched random field regime. By means of optic polarization spectroscopy they also show that the higher-temperature peak is related to the nucleation of nematic domains. This gives rise to a coarse-grained appearance of the sample. Surprisingly,

the lower-temperature peak exhibits a finer-grain texture. They claim that the finer texture arises due to the appearance of new domains and that the existing domains become broken into smaller one. The observed feature can be also explained using our approach. Namely, we show that at the phase transition region two different solutions exist, separated by a first-order phase transition. The finer optical structure could be explained by the appearance of multidomain structure, which arises due to the complex interaction between the phase separation and random-type field disorder within the system.

ACKNOWLEDGMENTS

V.P.N. acknowledges support from CNCSIS and CEEX (SIDISANIZ) grants. The authors acknowledge financial support from Ministries of Research and Education from Slovenia and Romania.

[1] *Liquid Crystals in Complex Geometries Formed by Polymer and Porous Networks*, edited by G. P. Crawford and S. Žumer (Taylor & Francis, London, 1996).
[2] T. Bellini, L. Radzihovsky, J. Toner, and N. A. Clark, Science **294**, 1074 (2001).
[3] T. Shinbrot and F. J. Muzzio, Nature (London) **410**, 251 (2001).
[4] M. V. Kurik and O. D. Lavrentovich, Sov. Phys. Usp. **31**, 196 (1988).
[5] T. Bellini, M. Buscaglia, C. Chiccoli, F. Mantegazza, P. Pasini, and C. Zannoni, Phys. Rev. Lett. **88**, 245506 (2002).
[6] N. A. Clark, T. Bellini, R. M. Malzbender, B. N. Thomas, A. G. Rappaport, C. D. Muzny, D. W. Schaefer, and L. Hrubesh, Phys. Rev. Lett. **71**, 3505 (1993).
[7] F. M. Aliev and M. N. Breganov, Zh. Eksp. Teor. Fiz. **95**, 122 (1989) [Sov. Phys. JETP **68**, 70 (1989)].
[8] G. S. Iannacchione, G. P. Crawford, S. Žumer, J. W. Doane, and D. Finotello, Phys. Rev. Lett. **71**, 2595 (1993).
[9] M. D. Dadmun and M. Muthukumar, J. Chem. Phys. **98**, 4850 (1993).
[10] Z. Kutnjak, S. Kralj, G. Lahajnar, and S. Žumer, Phys. Rev. E **70**, 051703 (2004).
[11] G. S. Iannacchione, C. W. Garland, J. T. Mang, and T. P. Rieker, Phys. Rev. E **58**, 5966 (1998).
[12] G. Cordoyiannis, G. Nounesis, V. Bobnar, S. Kralj, and Z. Kutnjak, Phys. Rev. Lett. **94**, 027801 (2004).
[13] G. P. Sinha and F. M. Aliev, Phys. Rev. E **58**, 2001 (1998).
[14] D. delas Heras, E. Velasco, and L. Mederos, Phys. Rev. Lett. **94**, 017801 (2005).
[15] D. J. Cleaver, S. Kralj, T. J. Sluckin, and M. P. Allen, in *Liquid Crystals in Complex Geometries Formed by Polymer and Porous Networks*, edited by G. P. Crawford and S. Žumer (Oxford University Press, London, 1996), p. 467.
[16] V. Popa-Nita, Eur. Phys. J. B **12**, 83 (1999).
[17] V. Popa-Nita and S. Romano, Chem. Phys. **264**, 91 (2001).
[18] S. Kralj and V. Popa-Nita, Eur. Phys. J. E **14**, 115 (2004).
[19] Y. Imry and S. Ma, Phys. Rev. Lett. **35**, 1399 (1975).
[20] J. Chakrabarti, Phys. Rev. Lett. **81**, 385 (1998).
[21] D. E. Feldman, Phys. Rev. Lett. **84**, 4886 (2000); Int. J. Mod. Phys. B **15**, 2945 (2001).
[22] T. Giamarchi and P. Le Doussal, Phys. Rev. B **52**, 1242 (1995).
[23] B. Zhou, G. S. Iannacchione, C. W. Garland, and T. Bellini, Phys. Rev. E **55**, 2962 (1997).
[24] V. J. Anderson, E. M. Terentjev, S. P. Meeker, J. Crain, and W. C. K. Poon, Eur. Phys. J. E **4**, 11 (2001).
[25] V. Popa-Nita, T. J. Sluckin, and S. Kralj, Phys. Rev. E **71**, 061706 (2005).
[26] N. F. Carnaham and K. E. Starling, J. Chem. Phys. **51**, 635 (1969).
[27] P. J. Flory, *Principles of Polymer Chemistry* (Cornell University Press, Ithaca, NY, 1953).
[28] V. Popa-Nita and S. Kralj, Phys. Rev. E **71**, 042701 (2005).
[29] R. Harris, M. Plischke, and M. J. Zuckermann, Phys. Rev. Lett. **31**, 160 (1973).
[30] P. G. de Gennes and J. Prost, *The Physics of Liquid Crystals* (Oxford University Press, Oxford, 1993).
[31] T. Bellini, M. Buscaglia, C. Chiccoli, F. Mantegazza, P. Pasini, and C. Zannoni, Phys. Rev. Lett. **85**, 1008 (2000).
[32] P. A. Lebwohl and G. Lasher, Phys. Rev. A **6**, 426 (1972).
[33] P. Oswald and P. Pieranski, *Les Cristaux Liquides: Concepts et Propriétés Physiques Illustrés par des Expériences* (Gordon and Breach, Amsterdam, 2000), Vol. 1.
[34] R. L. Humphries, P. J. James, and G. R. Luckhurst, J. Chem. Soc., Faraday Trans. 2 **68**, 1031 (1972).
[35] J. Katriel, G. F. Kventsel, G. R. Luckhurst, and T. J. Sluckin, Liq. Cryst. **1**, 337 (1986).
[36] A. Poniewierski and T. J. Sluckin, Liq. Cryst. **2**, 281 (1987).
[37] P. M. Chaikin and T. C. Lubensky, *Principles of Condensed Matter Physics* (Cambridge University Press, Cambridge, England, 1995).
[38] M. Kleman and O. D. Lavrentovich, *Soft Matter Physics, an Introduction* (Springer, Berlin, 2002).
[39] Z. Bradač, S. Kralj, and S. Žumer, Phys. Rev. E **65**, 021705 (2002), and references therein.
[40] E. M. Chudnovsky, W. M. Saslow, and R. A. Serota, Phys. Rev. B **33**, 251 (1986).
[41] F. Mercuri, S. Paoloni, U. Zammit, and M. Marinelli, Phys. Rev. Lett. **94**, 247801 (2005).
[42] M. Marinelli, F. Mercuri, S. Paoloni, and U. Zammit, Phys. Rev. Lett. **95**, 237801 (2005).